JPn Neuroscience

The Journal of Physiology

J Physiol 591.4 (2013) pp 1001–1015

CLC-3 chloride channels moderate long-term potentiation at Schaffer collateral–CA1 synapses

Laurel M. Farmer, Brandy N. Le and Deborah J. Nelson

Department of Neurobiology, Pharmacology and Physiology, The University of Chicago, Chicago, IL 60637, USA

Key points

- The CLC-3 chloride channel is expressed on postsynaptic membranes, where it is spatially and functionally linked to the NMDA receptor.
- CLC-3 is phosphorylated by Ca^{2+}/calmodulin kinase II.
- Loss of CLC-3 expression or prevention of CLC-3 phosphorylation/gating results in excessive induction of long-term potentiation.
- Given that knockout of CLC-3 results in hippocampal neurodegeneration, our results suggest that CLC-3 gating may provide a protective limit on plasticity and Ca^{2+} influx.

Abstract The chloride channel CLC-3 is expressed in the brain on synaptic vesicles and postsynaptic membranes. Although CLC-3 is broadly expressed throughout the brain, the CLC-3 knockout mouse shows complete, selective postnatal neurodegeneration of the hippocampus, suggesting a crucial role for the channel in maintaining normal brain function. CLC-3 channels are functionally linked to NMDA receptors in the hippocampus; NMDA receptor-dependent Ca^{2+} entry, activation of Ca^{2+}/calmodulin kinase II and subsequent gating of CLC-3 link the channels via a Ca^{2+}-mediated feedback loop. We demonstrate that loss of CLC-3 at mature synapses increases long-term potentiation from $135 \pm 4\%$ in the wild-type slice preparation to $154 \pm 7\%$ above baseline ($P < 0.001$) in the knockout; therefore, the contribution of CLC-3 is to reduce synaptic potentiation by ~40%. Using a decoy peptide representing the Ca^{2+}/calmodulin kinase II phosphorylation site on CLC-3, we show that phosphorylation of CLC-3 is required for its regulatory function in long-term potentiation. CLC-3 is also expressed on synaptic vesicles; however, our data suggest functionally separable pre- and postsynaptic roles. Thus, CLC-3 confers Cl^- sensitivity to excitatory synapses, controls the magnitude of long-term potentiation and may provide a protective limit on Ca^{2+} influx.

(Received 23 August 2012; accepted after revision 15 November 2012; first published online 19 November 2012)
Corresponding author D. J. Nelson: The University of Chicago, Department of Neurobiology, Pharmacology and Physiology, 947 East 58th Street, Chicago, IL 60637, USA. Email: nelson@uchicago.edu

Abbreviations CaM, calmodulin; CaMKII, Ca^{2+}/calmodulin kinase II; DIC, differential interference contrast; fEPSP, field excitatory postsynaptic potential; ISI, interstimulus interval; KCC2, K^+–Cl^- cotransporter; KO, knockout; LTP, long-term potentiation; NMDAR, NMDA receptor; NR1, NMDA receptor subunit 1; PFA, paraformaldehyde; PPF, paired-pulse facilitation; PSD, postsynaptic density; SK channel, small-conductance Ca^{2+}-activated K^+ channel; VGLUT1, vesicular glutamate transporter 1; WT, wild-type.

Introduction

The chloride channel CLC-3 is expressed in the brain on synaptic vesicles (Stobrawa *et al.* 2001) and postsynaptic plasma membranes (Wang *et al.* 2006). Although CLC-3 is broadly expressed throughout the brain (Kawasaki *et al.* 1994), the CLC-3 knockout mouse shows complete, selective postnatal neurodegeneration of the hippocampus (and photoreceptors). Similar neurodegeneration has been documented in the three *Clcn3*$^{-/-}$ mice that have been made and can be seen over a time period of 7 months in the hippocampus of the *Clcn3*$^{-/-}$ mice in

DOI: 10.1113/jphysiol.2012.243485

this study. The apparent hippocampal sensitivity to CLC-3 loss, in combination with the synaptic localization and previously demonstrated role in modulating synaptic events, motivated our investigation into the function of CLC-3 in controlling plasticity at the CA3–CA1 synapse (Stobrawa *et al.* 2001; Dickerson *et al.* 2002; Yoshikawa *et al.* 2002).

The Cl^- gradient, often through the employment of CLC channels and transporters, is a key determinant of cell excitability over short time scales, such as during bursts of inhibitory network activity, and over extended time scales throughout development (Ben-Ari *et al.* 1989, 1997; Ben-Ari, 2002). Underscoring the importance of the Cl^- ion in cell function, five of the nine CLC Cl^- channel family members have so far been linked to human diseases, such as myotonia (CLC-1), Bartter syndrome (CLC-Kb) and Dent's disease (CLC-5). Additionally, decreased expression of K^+–Cl^- cotransporter KCC2, the primary extruder of Cl^- in mature neurons, is associated with ischaemic brain injury and seizures (Jin *et al.* 2005; Pathak *et al.* 2007; Papp *et al.* 2008). Changes in KCC2 expression can be induced by NMDA receptor (NMDAR) activity, resulting in depolarizing $GABA_A$ receptor currents (Lee *et al.* 2011). Although it is apparent that excitatory synaptic activity can indirectly affect inhibition via $[Cl^-]_i$, a role for Cl^- in directly altering excitatory synaptic responses is relatively unexplored.

The Cl^- ion is also critically involved in volume regulation and is the primary charge shunt conductance utilized in intracellular organelles. In the brain, presynaptic CLC-3 was shown to aid synaptic vesicle acidification (Stobrawa *et al.* 2001; Riazanski *et al.* 2011); however, the necessity of CLC-3 as the glutamatergic vesicular shunt pathway is debated owing to an apparent Cl^- flux through the glutamate transporter VGLUT1 (Schenck *et al.* 2009). Conversely, at inhibitory synapses CLC-3 serves as the primary charge shunt pathway to facilitate neurotransmitter loading (Riazanski *et al.* 2011). Vesicular CLC-3 activation is likely to be gated by changes in intravesicular pH, driven by the vesicular ATPase (Matsuda *et al.* 2008*b*). Plasma membrane CLC-3 is unique among its family members in that it is gated by Ca^{2+}-dependent phosphorylation (Huang *et al.* 2001; Robinson *et al.* 2004; Wang *et al.* 2006). NMDAR-dependent Ca^{2+} entry, activation of Ca^{2+}/calmodulin kinase II (CaMKII) and subsequent phosphorylation/gating of CLC-3 by CaMKII link the two channels via a Ca^{2+}-mediated feedback loop. Two major splice variants of CLC-3, CLC-3A and CLC-3B, have differential expression profiles with regard to both tissue type and subcellular localization to organelles or the plasma membrane (Gentzsch *et al.* 2002; Ogura *et al.* 2002; Zhao *et al.* 2007); the reliance on pH *versus* CaMKII phosphorylation for gating is potentially explained by inherent differences in isoform structure or divergent trafficking. As a result of the shift in the Cl^- gradient during development (Ben-Ari *et al.* 1989, 1997; Ben-Ari, 2002; Jentsch *et al.* 2005), plasma membrane CLC-3 promotes depolarization in immature neurons and suppresses excitability in mature neurons when Cl^- flux is inhibitory (Wang *et al.* 2006). Thus, in the mature brain, CLC-3 channels serve as a charge shunt pathway, giving rise to membrane hyperpolarization, reduction in excitatory current amplitude and promotion of the block of NMDARs by Mg^{2+}.

Long-term potentiation (LTP) at the Schaffer collateral–CA1 synapse in the hippocampus is dependent on Ca^{2+} entry through NMDARs (Lynch *et al.* 1983; Kauer *et al.* 1988; Malenka *et al.* 1988; Malenka & Nicoll, 1993). Influx of Ca^{2+} activates protein kinases, such as CaMKII, that act to increase the sensitivity of the postsynaptic cell to glutamate release via AMPA receptor insertion (Shi *et al.* 1999; Bredt & Nicoll, 2003; Collingridge *et al.* 2004), phosphorylation (Benke *et al.* 1998; Derkach *et al.* 1999; Lee *et al.* 2003) or immobilization in the postsynaptic density (PSD; Bats *et al.* 2007; Opazo *et al.* 2010). The tight functional and spatial coupling of CLC-3 and synaptic NMDARs demonstrated by Wang *et al.* (2006) suggests that CLC-3 acts essentially as a biophysical property of the NMDAR; the receptor is functionally sensitive to the Cl^- gradient, without a literal Cl^- conductance of its own. Neuronal Cl^- homeostasis is a fundamental determinant of excitability in the brain; thus, we investigated the ability of CLC-3 to regulate synaptic plasticity in the hippocampus. Given that there is no specific antagonist of CLC-3, we used a *Clcn3*$^{-/-}$ mouse model for our studies (Dickerson *et al.* 2002).

Methods

Ethical approval

Studies were performed according to the principles set forth by the Animal Welfare Act and Guide for the Care and Use of Laboratory Animals published by the US National Institutes of Health (NIH publication no. 85-23, revised 1996) and were approved by the University of Chicago Institutional Animal Care and Use Committee.

Slice preparation

We used *Clcn3*$^{-/-}$ (KO) mice (Dickerson *et al.* 2002) and littermate wild-type (WT) mice as control animals. Genotyping was performed as previously described (Dickerson *et al.* 2002; Wang *et al.* 2006) by Transnetyx (Cordova, TN, USA). Mice were anaesthetized using isofluorane and rapidly decapitated using a guillotine. Brains were removed and horizontal hippocampal slices (350 μm) prepared from juvenile mice (postnatal day 19–30) in ice-cold dissection solution. Slices

were incubated at room temperature for at least 2 h in oxygenated (95% O_2 and 5% CO_2) artificial cerebrospinal fluid containing (mM): 126 NaCl, 2.5 KCl, 1.25 NaH_2PO_4, 26 $NaHCO_3$, 2.5 $CaCl_2$, 1.5 $MgCl_2$ and 10 glucose. In experiments with Tat-peptides, 5 or 10 μM Tat-peptide was added to the incubation chamber. Tat-CLC-$3_{107-116}$ (YGRKKRRQRRR-INSKKKESAW) and Tat-CLC-3_{scr} (YGRKKRRQRRR-KSIESANKWK) were obtained from GenScript (Piscataway, NJ, USA).

Electrophysiology

Extracellular field recordings were performed in an interface chamber at 32°C using an EPC9 patch-clamp amplifier (HEKA, Bellmore, New York, USA). Extracellular recording pipette (4–6 MΩ) solution contained artificial cerebrospinal fluid as above. Recordings were low-pass filtered at 2.8 kHz with an eight-pole Bessel filter and digitized at 10 kHz. A theta burst stimulation protocol was used to induce LTP (Albensi *et al.* 2007), which was maintained for at least 50 min after induction.

Immunohistochemistry

Brain tissues from two postnatal day 42 WT and *Clcn3*$^{-/-}$ mice were transcardially perfused and fixed with 4% paraformaldehyde (PFA). Brain tissues were cryoprotected in 30% sucrose solution overnight and further postfixed overnight in 4% PFA at 4°C. The brain was embedded and frozen in cryo-optimal temperature cutting compound (Electron Microscopy Sciences, Hatfield, PA, USA) and cut into serial cryosections (50 μm). For labelling of synaptic proteins, slices were rinsed with PBS and permeabilized with TritonX-100 (0.25%) for 5 min at room temperature. Non-specific binding sites were blocked in PBS blocking solution containing normal goat serum (5%) and bovine serum albumin (1%) for 30 min. Slices were incubated at room temperature for 1 h with the following primary antibodies diluted in blocking solution: rabbit α-CLC-3 (1:100 dilution; Alomone, Jerusalem, Israel) plus mouse monoclonal α-NR1 (1:100 dilution; Abcam, Cambridge, MA, USA) or goat polyclonal α-PSD-95 (1:100 dilution; Abcam). Primary antibody binding was amplified and visualized with Dylight 488-conjugated goat α-rabbit antibody (1:250 dilution; Abcam) for α-CLC3 and Alexa 633-conjugated goat α-mouse or donkey α-goat antibody (1:250 dilution; Abcam) for α-NMDA receptor subunit 1 (α-NR1) and PSD-95, respectively, for 30 min at room temperature. Coverslips were mounted and examined with a Leica SP5 confocal microscope at ×63 magnification with ×4 zoom.

For staining of CLC-3-expressing tsA cells (human embryonic kidney cells transformed with the SV40 Large T-antigen), the stably transfected or mock-transfected cells were washed three times with ice-cold PBS and fixed in 4% paraformaldehyde for 10 min at room temperature. Cells were then permeabilized with 0.2% Tween-20 in PBS for 30 min at room temperature. After 1 h in blocking buffer, cells were incubated with a rabbit α-CLC-3 antibody (Alomone) at 1:100 dilution for 2 h at room temperature. Cells were then washed with PBS and incubated with AlexaFluor 488-conjugated goat α-rabbit IgG (Invitrogen, Grand Island, NY, USA) for 1 h. Mock-transfected cells were used as controls. The coverslips were mounted on a slide and observed using confocal microscopy (Olympus Fluoview).

Cell culture/protein expression

CLC-3 expressing tsA cells and mock-transfected tsA cells were used according to Huang *et al.* (2001). Stably transfected clonal cell lines were maintained using zeocin (Invitrogen) at 200 μg ml^{-1}.

Preparation of autonomous CaMKII

Ten microlitres of CaMKII (1 mg ml^{-1}; purified from rodent brain; gift from Dr Andrew Hudman at the University of Indiana) were incubated with 2 μl calmodulin (1 mg ml^{-1}) and 8 μl autophosphorylation cocktail (2 mM $CaCl_2$, 25 mM $MgCl_2$, 2 mM ATPγS and 125 mM Tris–HCl, pH 7.4) at room temperature for 10 min. For peptide phosphorylation studies, the mixture was dialysed with 1× CaMKII reaction buffer using 30,000 molecular weight cut-off centrifugal filter apparatus. Buffer exchange was repeated three times to eliminate autophosphorylation cocktail and calmodulin.

Phosphorylation of synthetic peptides by CaMKII

Reaction mixtures were prepared in triplicate and consisted of 1× reaction buffer plus 50 μM peptide, 200 μM Mg-ATP, 125 μCi ml^{-1} [γ-^{32}P]ATP (PerkinElmer, Waltham, Massachusetts, USA) and 2 μl diluted kinase (added last). The total reaction volume was 30 μl. Upon addition of kinase, tubes were incubated for 30 min at 30°C. After incubation, reaction mixtures were spotted onto labelled P81 phosphocellulose squares (Millipore, Billerica, MA, USA) and dropped into ice-cold 75 mM phosphoric acid wash buffer to terminate the reaction and wash away unbound ATP. The P81 squares were washed with wash buffer, dipped briefly in acetone, dried, and then placed in individual scintillation vials. Radioactivity was measured in a scintillation counter (Cherenkov counting).

Immunoprecipitation and Western blot

tsA cells stably transfected with CLC-3 were solubilized in modified RIPA buffer (150 mM NaCl, 10 mM

$NaPO_4$, pH 7.4, 1% Triton X-100, 0.1% SDS and 2 mM EDTA) with protease inhibitors (1:200 dilution; Sigma-Aldrich, St. Louis, MO, USA). Fifty microlitres of protein A-conjugated magnetic Dynabeads (Invitrogen) was incubated with 5 μl α-CLC-3 (Alomone) for 10 min at room temperature with rotation and used to immunoprecipitate CLC-3 from the cell lysate at room temperature for 1 h. Following three washes with PBS, CLC-3 was eluted with Western blot sample buffer (200 mM Tris-HCl, pH 6.8, 8% SDS, 40% glycerol, 50 mM EDTA and 100 mM DTT). For phosphorylation experiments, the precipitated CLC-3 was incubated with 50 μl of CaMKII reaction mixture (2 μg CaMKII, 5 mM $CaCl_2$, 3 μg calmodulin and 5 mM Mg-ATP) at room temperature for 30 min before elution. The phosphorylation reaction was terminated, protein eluted, and resolved by 4–20% SDS-PAGE (Bio-Rad, Hercules, CA, USA). The resulting bands on the gel were detected using HRP-conjugated secondary antibody with enhanced chemiluminescence (Thermo Scientific, Waltham, MA, USA).

Neuron cultures

Hippocampal neurons for testing Tat-peptide uptake, a kind gift from Dr Jeremy Marks at the University of Chicago, were prepared from mice on postnatal day 5. Neurons were sparsely plated (1×10^4 neurons per dish) on no. 1.5 thickness coverglass to allow clear visualization of individual processes. Neurons were maintained in Neurobasal-A Medium supplemented by 2% B-27 Serum-Free Supplement (50×) and 0.5 mM GlutaMAX. Cultures were maintained for 1–2 weeks in culture before experiments were performed. All supplies were from Invitrogen.

Data analysis

Unless otherwise indicated, all data in this study are reported as mean values ± SEM with the number of slices in parentheses. Confidence was assessed by Student's paired or unpaired *t* test between data sets using OriginPro 8.2 (Northampton, MA, USA) as indicated in the figure legends.

Results

CLC-3 and NMDARs colocalize in the PSD of CA1 neurons

Previous studies have demonstrated that CLC-3 localizes to the postsynaptic plasma membrane of excitatory synapses in cultured hippocampal neurons (Wang *et al.* 2006). Using confocal microscopy on fixed hippocampal slices, we labelled WT and *Clcn3*$^{-/-}$ slices with an antibody to CLC-3 (Fig. 1*A*). CLC-3 was expressed in WT slices throughout the CA1 region of the hippocampus in both the cell body layer and the dendrites, while *Clcn3*$^{-/-}$ sections showed no specific labelling. We next co-labelled the sections for CLC-3 and either the NR1 subunit of the NMDAR or the postsynaptic density protein PSD-95 (Fig. 1*B*). We found a high degree of overlap of CLC-3 with NR1 and PSD-95 in the stratum radiatum of CA1 (Fig. 1*B*). Quantitative analysis of the fluorescence signals revealed correlation coefficients of 0.80 and 0.84 for CLC-3 with PSD-95 and NR1, respectively, reflecting the precise spatial correlation of the proteins.

CLC-3 regulates the magnitude of LTP at Schaffer collateral–CA1 synapses

Long-term potentiation at the Schaffer collateral–CA1 synapse in the hippocampus is dependent on Ca^{2+} entry through NMDARs (Lynch *et al.* 1983; Kauer *et al.* 1988; Malenka *et al.* 1988; Malenka & Nicoll, 1993). Based on the functional and spatial coupling of CLC-3 with NMDARs, we investigated a role for CLC-3 in modulating LTP in the hippocampus.

Extracellular recording was used to preserve the endogenous Cl^- gradient, crucial for interpreting the role of E_{Cl} in synaptic plasticity. Recording electrodes were placed in the CA1 stratum radiatum of hippocampal slices from postnatal day 19–30 *Clcn3*$^{-/-}$ and WT mice. Field excitatory postsynaptic potentials (fEPSPs) were evoked by stimulating the Schaffer collaterals with a bipolar electrode. An input–output curve was measured to assay baseline neurotransmission, and the stimulus intensity was set to evoke field responses that were 30% of the maximal fEPSP amplitude (Fig. 2*A*). Although *Clcn3*$^{-/-}$ slices trended towards higher stimulation intensities (Fig. 2*A* left panel, WT, 74 ± 13 μA, $n = 10$; and KO, 124 ± 22 μA, $n = 8$; $P = 0.06$) and decreased maximal responses (Fig. 2*A* right panel, WT, 1.86 ± 0.18 mV, $n = 10$; and KO, 1.58 ± 0.13 mV, $n = 8$; $P > 0.05$), possibly a harbinger of impending neurodegeneration, neither parameter was significantly different between WT and *Clcn3*$^{-/-}$ slices.

Long-term potentiation was evoked using a theta burst stimulation protocol (Albensi *et al.* 2007) following a 20 min baseline period. After at least 50 min of stable LTP expression, we found that *Clcn3*$^{-/-}$ slices exhibited a 1.54 ± 7 ($n = 8$) fold-potentiation, significantly greater than the 1.35 ± 4 ($n = 10$) potentiation expressed by WT slices ($P < 0.001$; Fig. 2*B*). This result is consistent with prior studies showing that CLC-3 modulates synaptic events and evoked NMDAR currents in accordance with the Cl^- gradient (Wang *et al.* 2006); removal of the inhibitory Cl^- conductance allows for increased Ca^{2+} influx and, therefore, potentiation.

Paired-pulse facilitation is increased in *Clcn3*$^{-/-}$ slices

To control for changes in presynaptic function with LTP, we performed paired-pulse experiments before and after LTP. We measured fEPSPs 20 min before LTP induction in response to paired-pulse stimulation of the Schaffer collaterals at a range of interstimulus intervals (ISIs). Representative traces at ISI = 50 ms are shown in Fig. 3*A*, with data from all ISIs summarized in Fig. 3*B*. We observed robust paired-pulse facilitation (PPF) of the fEPSP in both WT and *Clcn3*$^{-/-}$ slices (PPF = amplitude of second/first peak; at 50 ms, WT, 1.60 ± 0.06, $n = 14$; and KO, 2.16 ± 0.09, $n = 8$), a well-characterized feature of the CA3–CA1 synapse (Zucker & Regehr, 2002; Ahmed & Siegelbaum, 2009). However, significantly greater PPF was measured in *Clcn3*$^{-/-}$ slices at all ISIs (Fig. 3*B*, $^{*}P < 0.01$ and $^{**}P < 0.001$, Student's unpaired *t* test).

We repeated the paired-pulse protocol 1 h after induction of LTP to test whether presynaptic responses were altered (Fig. 3*C*). At short ISIs, WT slices displayed a slight decrease in PPF ($n = 7$; ISI = 30–100 ms, $P < 0.05$), but no significant difference appeared at longer intervals (ISI = 150–200 ms, $P > 0.05$). Minimal changes in PPF are reported as a consequence of postsynaptically expressed LTP at the CA3–CA1 synapse (Kerchner & Nicoll, 2008), consistent with our measurements. The *Clcn3*$^{-/-}$ slices showed small, inconsistent changes in PPF across ISIs, but these were significant at only one interval ($n = 4$; ISI = 60 ms, $P < 0.05$; all other ISIs, $P > 0.05$). Although

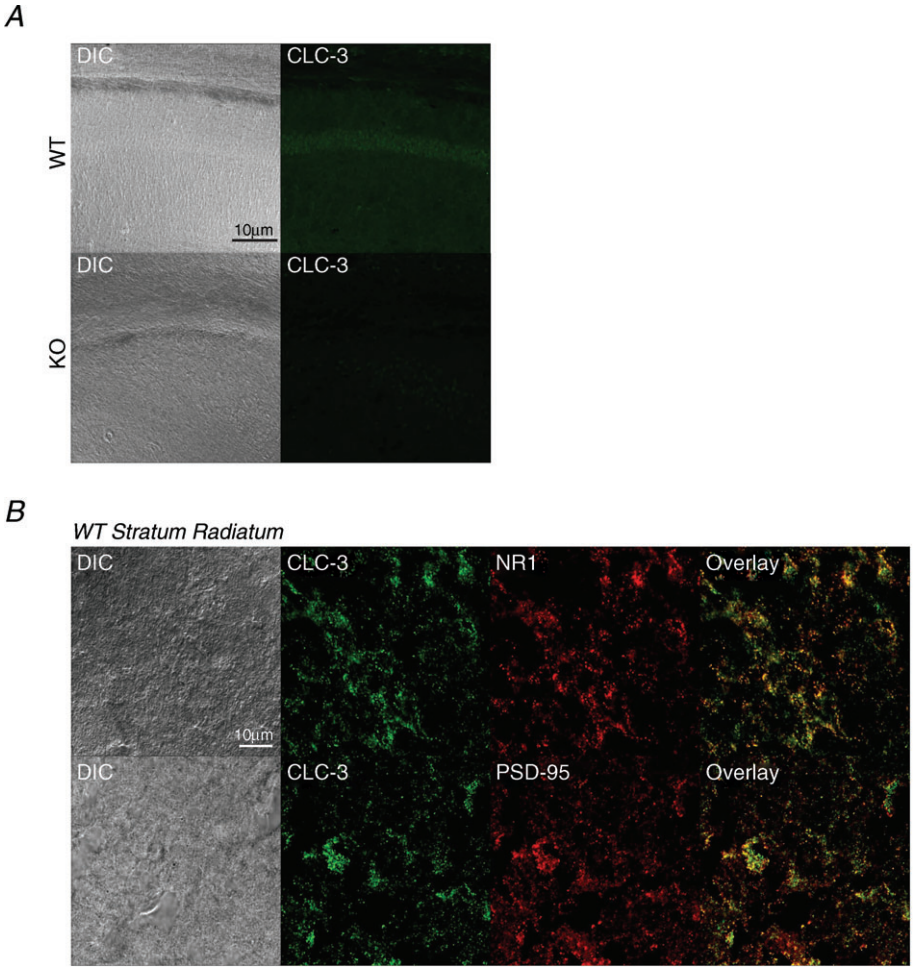

Figure 1. CLC-3 colocalizes with postsynaptic density 95 (PSD-95) and NMDA receptors (NMDARs) at postsynaptic sites
Cryosections were made from the hippocampus of postnatal day 42 wild-type (WT) and *Clcn3*$^{-/-}$ (KO) mice, stained for desired proteins, and imaged at ×63 magnification with ×4 zoom on a confocal microscope. *A*, CLC-3 is expressed throughout the CA1 region of the hippocampus in WT but not *Clcn3*$^{-/-}$ sections. *B*, CLC-3 immunostaining overlaps extensively with staining for the postsynaptic proteins NR1 and PSD-95 in the WT stratum radiatum. Manders' coefficients quantifying the degree of overlap are 0.82 for the fraction of NR1 overlapping CLC-3 and 0.70 for CLC-3 overlapping NR1, with a correlation coefficient of 0.84. The fraction of PSD-95 overlapping CLC-3 is 0.67 and CLC-3 overlapping PSD-95 is 0.80, with a correlation coefficient of 0.81. Qualitative analysis of colocalization was done using ImageJ plug-in JACoP (Fabrice *et al.* 2006).

loss of presynaptic CLC-3 has a striking effect on presynaptic function, presynaptic release is little changed by LTP induction in WT or *Clcn3*$^{-/-}$ slices.

CLC-3 is phosphorylated by CaMKII

Three putative CaMKII phosphorylation sites have been identified on CLC-3 (Kawasaki *et al.* 1994; Robinson *et al.* 2004). In order to examine phosphorylation of CLC-3 directly, we used a human embryonic kidney cell line derivative that was stably transfected with recombinant CLC-3 (tsA-CLC-3). Control experiments used tsA cells that were mock transfected with only a selection vector (tsA-mock). Figure 4*A* demonstrates strong expression of CLC-3 in tsA-CLC-3 cells and low basal expression in tsA-mock cells. Using an antibody directed against the intracellular C-terminal domain, we immunoprecipitated CLC-3 from tsA-CLC-3 lysate but not control lysate (Fig. 4*B*). We incubated the precipitated CLC-3 protein with autophosphorylated CaMKII. After phosphorylating to completion, the protein was eluted using sample buffer, and CLC-3 was resolved using SDS-PAGE. We assayed for phosphorylation using an antiphosphoserine antibody. With application of CaMKII, a distinct phosphorylation signal appeared at the molecular weight of CLC-3 that did not appear in the untreated immunoprecipitation lane or pre-immunoprecipitation lane (Fig. 4*C*).

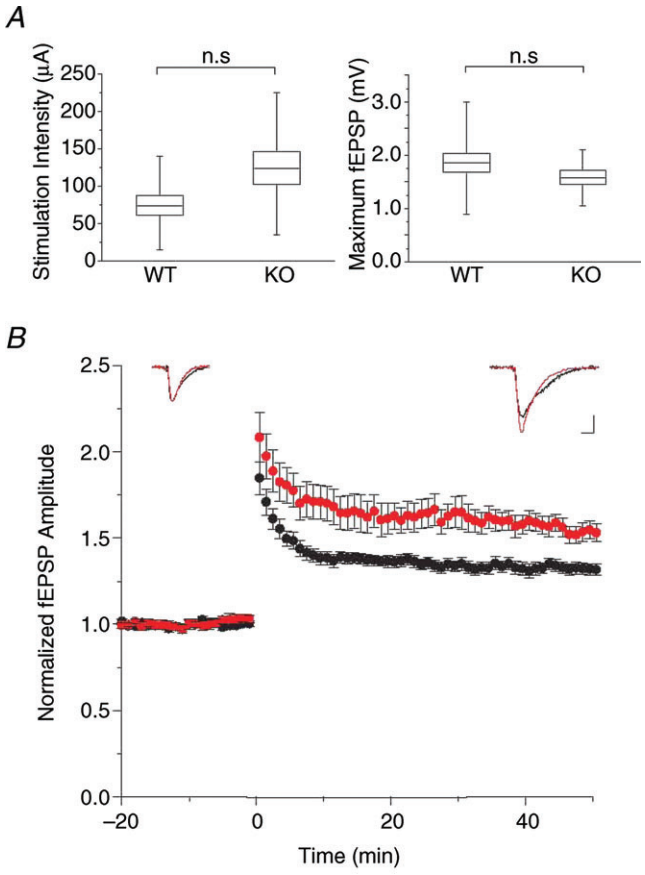

Figure 2. Long-term potentiation (LTP) is increased in *Clcn3*$^{-/-}$ slices
A, stimulation intensity (left panel) for WT (74 ± 13 μA, $n = 10$) and *Clcn3*$^{-/-}$ slices (124 ± 22 μA, $n = 8$, $P = 0.06$) required to produce a field excitatory postsynaptic potential (fEPSP) that is 30% of the maximal response (right panel; WT, 1.86 ± 0.18 mV, $n = 10$; and KO, 1.58 ± 0.13 mV, $n = 8$; $P > 0.05$). Box plots depict the mean (line across box), ± SEM (top and bottom of box) and range of the data. *B*, mean normalized fEPSP amplitude in response to theta burst stimulation at $t = 0$. Both WT (1.35 ± 4, $n = 8$) and *Clcn3*$^{-/-}$ slices (1.54±7, $n = 10$) show significant LTP at 50 min ($P < 0.001$, Student's paired *t* test). The *Clcn3*$^{-/-}$ (red traces and symbols) and WT slices (black traces and symbols) display significantly different magnitudes of LTP ($P < 0.001$, Student's unpaired *t* test). Each point is the mean ± SEM. Insets are averages of 10 fEPSPs (normalized to 1.0) for WT and *Clcn3*$^{-/-}$ slices before and after induction of LTP. Scale bar represents 0.5 and 10 ms.

Robinson *et al.* (2004) showed that mutation of serine 109 to alanine (S109A) prevented the CaMKII-activated Cl^- current in transiently transfected tsA cells, suggesting that plasma membrane CLC-3 is gated by CaMKII phosphorylation at S109. Thus, we hypothesized that by preventing CaMKII phosphorylation of CLC-3, we could mimic *Clcn3*$^{-/-}$ physiology in a WT preparation. Acute interference with CLC-3 function avoids developmental confounds of chronic genetic manipulation and secondary effects of the neurodegeneration associated with CLC-3 knockout.

There is no specific antagonist of CLC-3. We therefore used a strategy wherein we provided CaMKII with an alternative CLC-3-like target. We used the synthetic peptide CLC-$3_{107-116}$ (INSKKKESAW), representing amino acids 107−116 of the CLC-3 N-terminus and including S109, to titrate CaMKII activity from CLC-3. Synthetic peptides have previously been used to interfere with phosphorylation of endogenous ion channels involved in synaptic transmission (Ahmadian *et al.* 2004; Lin *et al.* 2008). The CLC-$3_{107-116}$ was made cell permeable by fusion to the human immunodeficiency virus type 1 Tat sequence (Tat-CLC-$3_{107-117}$; YGRKKRRQRRR-INSKKKESAW; Green & Loewenstein, 1988; Schwarze *et al.* 1999, 2000). Control experiments used Tat-CLC-3_{scr}, in which the Tat sequence remains but the subsequent residues are randomly arranged (Tat-CLC-3_{scr}; YGRKKRRQRRR-KSIESANKWK). Two different scrambled peptides were tested, with similar results. The Tat sequence has been used previously to introduce a peptide that disrupted a specific protein–protein interaction required for long-term depression (Ronesi & Huber, 2008).

We measured the ability of neurons to take up the peptide by conjugating Tat-CLC-3_{scr} to fluorescein. Cultured hippocampal neurons, used for improved visualization, displayed rapid uptake of the peptide, showing strong fluorescence after 15 min (Fig. 5*A*). We next tested whether the peptides could be phosphorylated

by CaMKII *in vitro* (Fig. 5*B*). Tat-peptides were combined with ^{32}P-radio-labelled ATP and autophosphorylated CaMKII. Control samples did not contain peptide and were tested with and without CaMKII. All conditions were tested in triplicate. The reaction was stopped after 30 min, and radioactivity was counted using a scintillation counter. When the peptide substrate was omitted, a baseline of <100 counts per minute (c.p.m.) was observed with and without CaMKII (85 ± 13 c.p.m. with CaMKII; 80±4 c.p.m. without CaMKII; $P > 0.05$, Student's unpaired t test). In contrast, Tat-CLC-3$_{107-116}$ peptide was phosphorylated 12 times greater than baseline (1077 ± 51 c.p.m.; $P < 0.001$). Tat-CLC-3$_{scr}$ was also phosphorylated significantly over baseline (350 ± 33 c.p.m.; $P < 0.01$), but three times less than Tat-CLC-3$_{107-116}$ ($P < 0.001$).

Modulation of LTP by CLC-3 requires CaMKII phosphorylation

We next investigated the ability of the CLC-3 peptide to inhibit CLC-3 gating during LTP. We incubated slices with Tat-CLC-3$_{107-116}$ or scrambled peptide for at least 2 h prior to recording. Baseline synaptic transmission was not different between slices treated with Tat-CLC-3$_{107-116}$ or scrambled peptide, as indicated by the input–output relationship (Fig. 5*C*); neither the maximal response (WT + Tat-CLC-3$_{107-116}$, 2.19 ± 0.14 mV, $n = 6$; and WT + Tat-CLC-3$_{scr}$, 2.57 ± 0.16 mV, $n = 13$; $P > 0.05$) nor the stimulation intensity required to achieve 30% thereof (WT + 10 μM Tat-CLC-3$_{107-116}$, 118 ± 18 μA, $n = 6$; and WT + 10 μM Tat-CLC-3$_{scr}$, 105 ± 9 μA, $n = 13$; $P > 0.05$, Student's unpaired t test) differed between groups. The addition of Tat-peptides did not significantly change baseline synaptic transmission compared with WT slices alone ($P > 0.05$).

Treatment with Tat-CLC-3$_{107-116}$ increased the magnitude of LTP expressed in WT slices in a dose-dependent manner (Fig. 5*E*, from left to right: 1.33 ± 0.04, $n = 10$; 1.43 ± 0.06, $n = 4$; 1.55 ± 0.06, $n = 6$; and 1.58 ± 0.07, $n = 8$; $^{**}P < 0.01$, $^{***}P < 0.001$; Student's unpaired t test). At 10 μM, Tat-CLC-3$_{107-116}$ resulted in the same magnitude of LTP as in *Clcn3*$^{-/-}$ slices ($P > 0.05$). Application of 10 μM Tat-CLC-3$_{scr}$ to a WT slice resulted in LTP that was not significantly different from WT slices alone (1.35 ± 0.05, $n = 6$; $P > 0.05$, Student's unpaired t test), suggesting that S109 and the surrounding residues are critical for recognition of CLC-3 by CaMKII (Fig. 6*A*). In addition, Tat-CLC-3$_{107-116}$ did not affect LTP in *Clcn3*$^{-/-}$ slices (1.54 ± 0.10, $n = 5$; $P > 0.05$), providing further evidence of peptide specificity for disrupting primarily the CLC-3–CaMKII interaction (Fig. 6*B*, and summarized in Fig. 6*C*). These data show that there is no broad inhibition of CaMKII by the Tat-peptides; if this were the case, we would expect impaired LTP induction (Malenka *et al.* 1989; Lisman *et al.* 2002); however, the opposite response is evident in Fig. 5. Finally, equivalent baseline transmission between WT

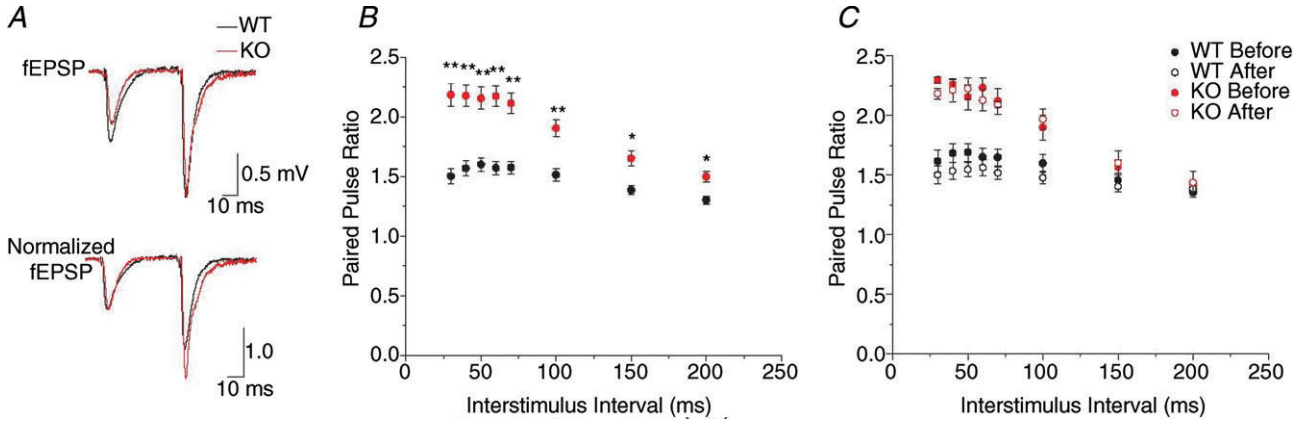

Figure 3. Paired-pulse facilitation (PPF) is increased in *Clcn3*$^{-/-}$ slices
A, field response in CA1 stratum radiatum to paired-pulse stimulation of the Schaffer collaterals. Stimulation intensity was adjusted to 30% of the maximal evoked response. Traces shown are at a 50 ms interstimulus interval (ISI) in WT (black traces) and *Clcn3*$^{-/-}$ slices (red traces). Top traces, average fEPSPs from six consecutive sweeps. Bottom traces, average fEPSPs normalized to the peak of the first fEPSP. *B*, paired-pulse ratios for WT and *Clcn3*$^{-/-}$ slices, calculated as the amplitude of second/first peak (at 50 ms, WT, 1.60 ± 0.06, $n = 14$; and KO, 2.16 ± 0.09, $n = 8$). The *Clcn3*$^{-/-}$ slices display significantly stronger facilitation at all intervals between 30 and 200 ms ($^{*}P < 0.01$, $^{**}P < 0.001$, Student's unpaired t test). *C*, paired-pulse stimulation before and following 50 min of stable LTP expression in WT ($n = 7$) and *Clcn3*$^{-/-}$ slices ($n = 4$). At short ISIs, WT slices displayed a slight decrease in PPF (ISI = 30–100 ms, $P < 0.05$, Student's paired t test), but no significant difference appeared at longer intervals (ISI = 150–200 ms, $P > 0.05$, Student's paired t test). The *Clcn3*$^{-/-}$ slices showed small, inconsistent changes in PPF across ISIs, but these were significant at only one interval (ISI = 60 ms, $P < 0.05$; all other ISIs, $P > 0.05$; Student's paired t test), suggesting postsynaptic expression of LTP. Each point is the mean ± SEM.

and Tat-peptide-treated slices further emphasizes that the acute effect of CLC-3 on LTP is dissociable from the long-term neurodegeneration phenotype.

Presynaptic release is unaffected by Tat-CLC-$3_{107-116}$

Both CaMKII and CLC-3 are expressed presynaptically as well as postsynaptically; CaMKII is involved in regulating presynaptic release (Wang, 2008; Pang *et al.* 2010), while vesicular CLC-3, at least in inhibitory vesicles, facilitates vesicle acidification and loading of neurotransmitter (Stobrawa *et al.* 2001; Schenck *et al.* 2009; Riazanski *et al.* 2011). It is possible that these proteins interact together presynaptically to increase vesicle release probability. We then would expect to see an increase in PPF with Tat-CLC-$3_{107-116}$ application to WT slices to match the PPF measured in *Clcn3*$^{-/-}$ slices. We repeated the paired-pulse protocol in all slices treated with Tat-peptides, but found the opposite result; presynaptic release properties followed the genotype of the preparation, unaltered by application of Tat-CLC-$3_{107-116}$ or Tat-CLC-3_{scr}. The *Clcn3*$^{-/-}$ slices treated with Tat-CLC-$3_{107-116}$ (50 ms ISI, 2.05 ± 0.15, $n = 5$) had increased PPF similar to *Clcn3*$^{-/-}$ slices without peptide (2.16 ± 0.09, $n = 8$; $P > 0.05$, Student's unpaired t test), while WT slices treated with Tat-CLC-$3_{107-116}$ (1.57 ± 0.04, $n = 6$) or Tat-CLC-3_{scr} (1.58 ± 0.06, $n = 6$) displayed WT PPF (1.60 ± 0.06, $n = 14$; $P > 0.05$ for both comparisons; Fig. 6*D*). The lack of peptide influence on presynaptic release suggests that the increase in PPF in *Clcn3*$^{-/-}$ slices is not due to a presynaptic interaction between CaMKII and CLC-3. Taken together, these data strongly suggest that CLC-3 is gated by CaMKII phosphorylation at the postsynaptic plasma membrane, not in presynaptic vesicles, and that this interaction is required for CLC-3 modulation of postsynaptically expressed LTP.

Discussion

Our data support a model of CLC-3 function presented in Fig. 7. Calcium ion influx through NMDARs

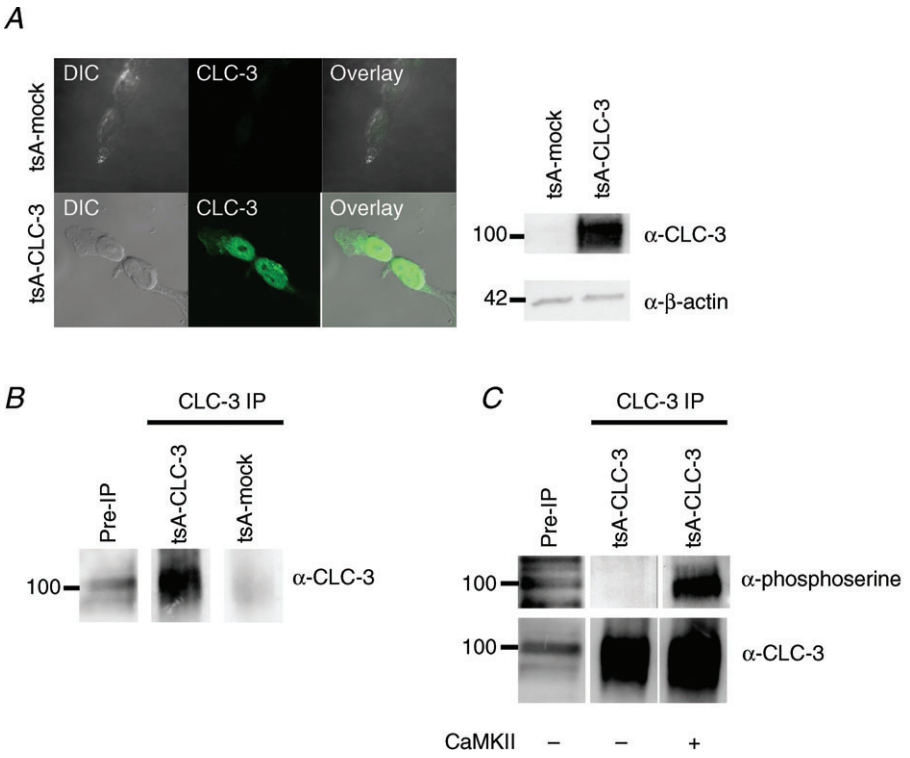

Figure 4. CLC-3 is phosphorylated by Ca^{2+}/calmodulin kinase II (CaMKII)
tsA cells were stably transfected with CLC-3 (tsA-CLC-3) or mock transfected with selection vector only (tsA-mock). *A*, tsA cells were fixed, permeablized, and labelled with an antibody to CLC-3. CLC-3 is expressed strongly in stably transfected tsA cells (bottom panels), while mock-transfected cells (top panels) have low endogenous expression. This is confirmed in a Western blot (right); tsA-mock cells do not show appreciable CLC-3 protein compared with tsA-CLC-3 cells. *B*, α-CLC-3 was incubated with protein A-conjugated magnetic Dynabeads and used to immunoprecipitate (IP) CLC-3 from tsA cells. We were able to immunoprecipitate CLC-3 from tsA-CLC-3 lysate but not from tsA-mock cells. *C*, CLC-3 is phosphorylated by CaMKII *in vitro*. Immunoprecipitated CLC-3 was incubated with activated CaMKII for 30 min, run out with SDS-PAGE, and probed for phosphorylation with an α-phosphoserine antibody. In the absence of kinase, there is negligible phosphorylation of the precipitated protein.

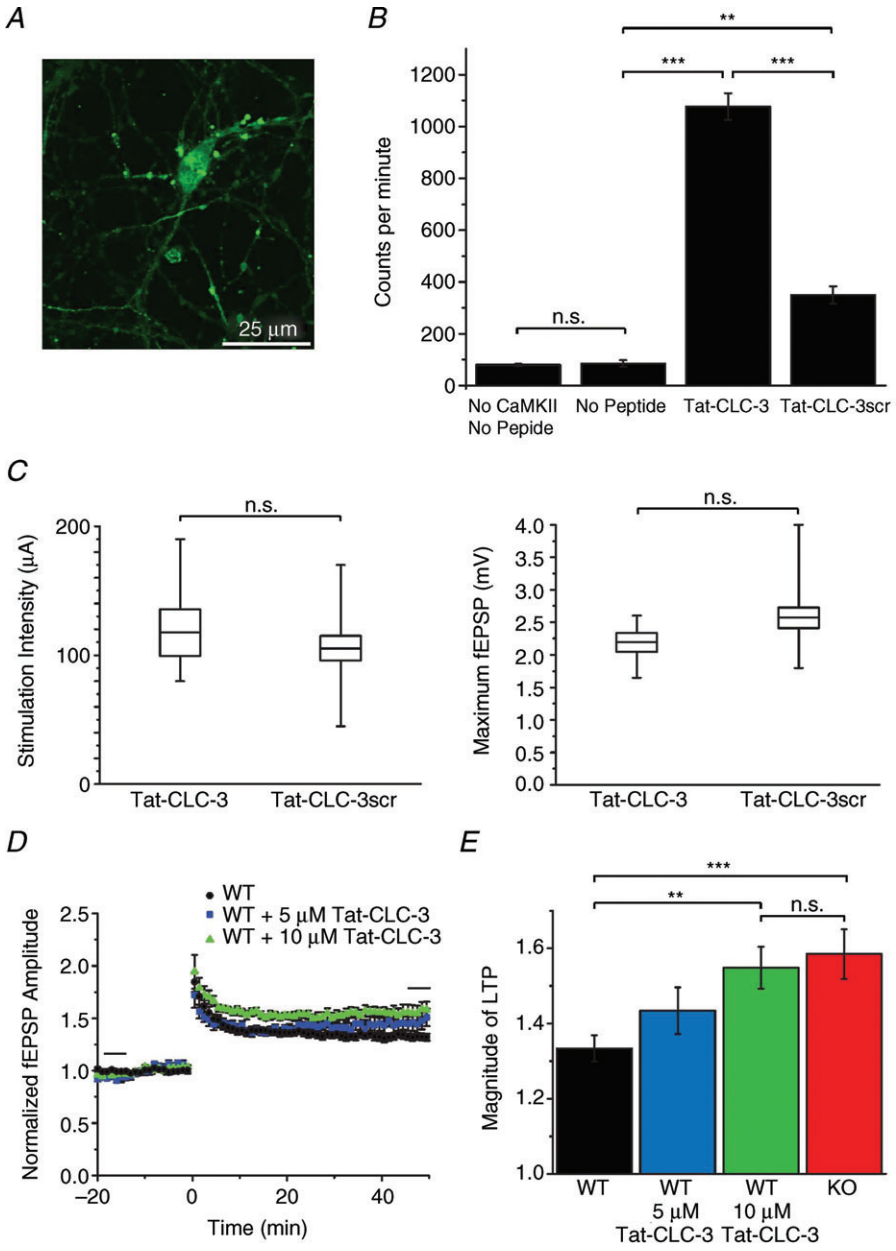

Figure 5. Application of the Tat-peptide Tat-CLC-$3_{107-116}$ to a WT slice mimics increased LTP in adult *Clcn3*$^{-/-}$ slices

A, uptake of fluorescein-labelled Tat-CLC-3_{scr} into cultured neurons. Cells displayed strong uptake within 15 min. *B*, *in vitro* phosphorylation of Tat-peptides by CaMKII using ^{32}P-labelled ATP. When kinase or peptides are not included in the reaction mixture, there is no difference in baseline counts per minute (80 ± 4 c.p.m., $n = 3$; 85 ± 13 c.p.m., $n = 3$; $P > 0.05$, Student's unpaired t test), measured by a scintillation counter. Addition of Tat-CLC-$3_{107-116}$ results in a 12-fold increase in ^{32}P counts (1077 ± 51 c.p.m., $n = 3$; $^{***}P < 0.001$) compared with the no-peptide condition. Scrambled peptide also increases ^{32}P counts from baseline (350 ± 33 c.p.m., $n = 3$; $^{**}P < 0.01$) but significantly less than Tat-CLC-$3_{107-116}$ ($^{***}P < 0.001$). All bars are the average of three experiments ± SEM. *C*, stimulation intensity (left) for WT slices with 10 μM Tat-CLC-$3_{107-116}$ (118 ± 18 μA, $n = 6$) and WT slices with 10 μM Tat-CLC-3_{scr} (105 ± 9 μA, $n = 13$; $P > 0.05$) required to produce an fEPSP that is 30% of the maximal response (right; Tat-CLC-$3_{107-116}$, 2.19 ± 0.14 mV, $n = 6$; and Tat-CLC-3_{scr}, 2.57 ± 0.16 mV, $n = 13$; $P > 0.05$). Two different scrambled peptides were tested with the same result, so these data are combined. Box plots depict the mean (line across box), ± SEM (top and bottom of box) and range of the data. Time course (*D*) and average magnitude of LTP (*E*) in WT slices with 0, 5 and 10 μM Tat-CLC-$3_{107-116}$ compared with *Clcn3*$^{-/-}$ slices (from left to right: 1.33 ± 0.04, $n = 10$; 1.43 ± 0.06, $n = 4$; 1.55 ± 0.06, $n = 6$; and 1.58 ± 0.07, $n = 8$; $^{**}P < 0.01$, $^{***}P < 0.001$, Student's unpaired t test). At 10 μM, Tat-CLC-$3_{107-116}$ produces LTP that is not significantly different from that in *Clcn3*$^{-/-}$ slices ($P > 0.05$).

activates CaMKII to initiate plasticity mechanisms, such as AMPA receptor insertion, to increase synaptic efficacy. Simultaneously, CaMKII enacts rapid measures to dampen Ca^{2+} influx by opening the Cl^- shunt conductance CLC-3 via S109 phosphorylation. CLC-3 negatively regulates further Ca^{2+} influx through the NMDAR and moderates the amount of plasticity expressed, thereby protecting active synapses from excitotoxicity.

In this study, we assayed the function of chloride channel CLC-3 at the postsynaptic membrane of excitatory synapses. Immunostaining in hippocampal slices demonstrated strong correlation of CLC-3 staining with postsynaptic markers NR1 and PSD-95, indicating spatial colocalization of the proteins (Fig. 1). Pixel-by-pixel comparison of the images revealed that CLC-3 staining overlapped spatially with the majority of both postsynaptic proteins. It has also been demonstrated that CLC-3 co-immunoprecipitates with NR1 and PSD-95 in isolated hippocampal neurons (Wang *et al.* 2006) and with CaMKII in human glioma cells (Cuddapah & Sontheimer, 2010). Plasma membrane CLC-3 is integrated into the postsynaptic density, where it cohabits in a microdomain with key structural and functional elements. These data advocate an important role for CLC-3 in determining the efficacy of synaptic transmission.

Prior work demonstrated tight functional coupling between CLC-3 and NMDARs, in which CLC-3 expression

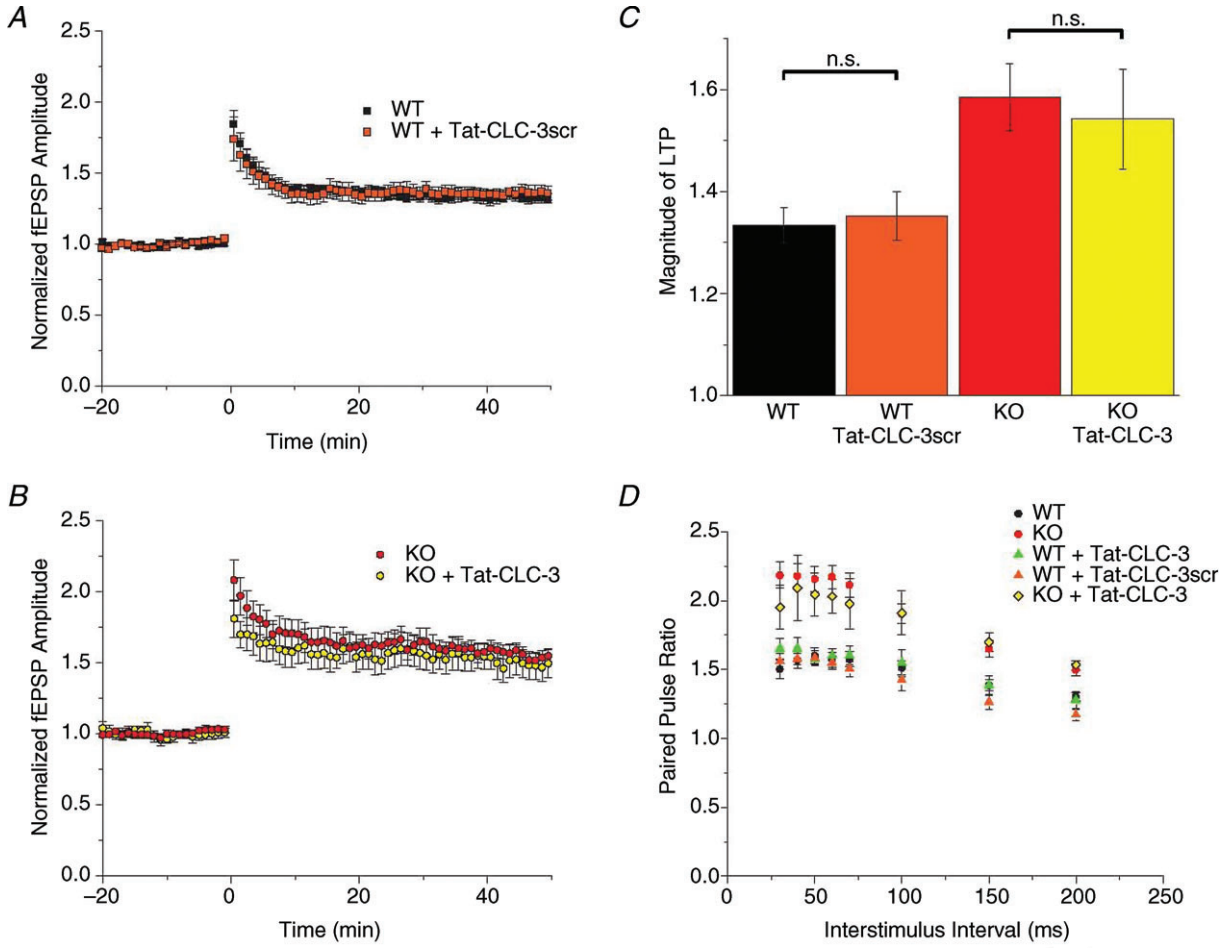

Figure 6. Tat-CLC-$3_{107-116}$ specifically blocks the postsynaptic interaction of CLC-3 and CaMKII
A, application of 10 μM Tat-CLC-3_{scr} to a WT slice results in LTP that is not significantly different from that in WT slices alone (1.35 ± 0.05, $n = 6$; $P > 0.05$, Student's unpaired *t* test). *B*, 10 μM Tat-CLC-$3_{107-116}$ does not alter *Clcn3*$^{-/-}$ LTP expression (1.54 ± 0.10, $n = 5$; $P > 0.05$), suggesting that it does not interfere with CaMKII phosphorylation of other substrates important for LTP. *C*, summary of LTP magnitudes in *A* and *B*, measured during the last 10 min of recording. *D*, presynaptic release is not significantly changed compared with WT slices alone (1.60 ± 0.06, $n = 14$) for WT slices with application of Tat-CLC-$3_{107-116}$ (1.57 ± 0.04, $n = 6$; $P > 0.05$) or Tat-CLC-3_{scr} (1.58 ± 0.06, $n = 6$; $P > 0.05$). In addition, facilitation measured in *Clcn3*$^{-/-}$ slices treated with Tat-CLC-$3_{107-116}$ (2.05 ± 0.15, $n = 5$) is not significantly different from *Clcn3*$^{-/-}$ slices alone (2.16 ± 0.09, $n = 8$; $P > 0.05$), suggesting a purely postsynaptic action of Tat-CLC-$3_{107-116}$ on LTP. Comparisons (Student's unpaired *t* test) were carried out for all ISIs, but reported for only ISI = 50 ms for brevity.

shifted the apparent NMDAR reversal potential negatively, from $E_{NMDAR} \approx 0$ mV to $E_{NMDAR} = -20$ mV. In addition, Ca^{2+} influx is required for CLC-3 gating, demonstrated by use of the fast Ca^{2+} buffer BAPTA in the intracellular solution (Wang *et al.* 2006). Long-term potentiation and its dependence upon NMDAR-mediated Ca^{2+} entry (Lynch *et al.* 1983; Kauer *et al.* 1988; Malenka *et al.* 1988) has been widely studied as a presumptive mechanism underlying learning and memory (Bliss & Collingridge, 1993; Reisel *et al.* 2002; Whitlock *et al.* 2006; Matsuo *et al.* 2008); however, despite the central role of Cl^- in synaptic inhibition, relatively little attention has been paid to the role of anion channels at excitatory synapses or in synaptic plasticity. Here we extend the repertoire of players in LTP to include CLC-3, unique in its ability to confer the NMDAR with a functional Cl^- sensitivity, which we propose is imperative for proper neuronal function and, ultimately, survival. Loss of CLC-3 expression or function (using Tat-CLC-$3_{107-116}$) at CA3–CA1 synapses results in significantly increased expression of LTP (Figs 2 and 5). Furthermore, CLC-3 is activated directly by CaMKII, the quintessential molecule responsible for induction of plasticity at multiple types of synapses in the brain by directing the distribution or biophysical properties of AMPA receptors (Benke *et al.* 1998; Derkach *et al.* 1999; Shi *et al.* 1999; Bredt & Nicoll, 2003; Lee *et al.* 2003; Collingridge *et al.* 2004).

Calcium transients last hundreds of milliseconds, but CaMKII activation extends for several seconds after the transient is complete (Lee *et al.* 2009). Consequently, CLC-3 gating is likely to extend beyond the NMDAR Ca^{2+} signal itself in order to influence subsequent synaptic events. A similar Ca^{2+}-mediated feedback loop at the synapse has been described involving small-conductance Ca^{2+}-activated K^+ channels (SK channels; Ngo-Anh *et al.* 2005; Lin *et al.* 2008; Lee *et al.* 2011). The SK2 channels are removed from the plasma membrane by protein kinase A-dependent endocytosis following LTP (Ngo-Anh *et al.* 2005; Lin *et al.* 2008). Lin *et al.* (2008) suggest that elimination of the SK2 conductance would remove inhibition of Ca^{2+} influx after induction of LTP, but this may be compensated through other homeostatic mechanisms. Given that CLC-3 is regulated in an activity-dependent fashion (increased Ca^{2+} influx is communicated to CLC-3 via CaMKII activity), CLC-3 is a candidate for such a homeostatic role. Removal of SK2 channels was estimated to be responsible for 13% of LTP induced (Lin *et al.* 2008). We found that loss of CLC-3 expression or gating nearly doubles LTP from 33% above baseline to 58%; therefore, we estimate that the

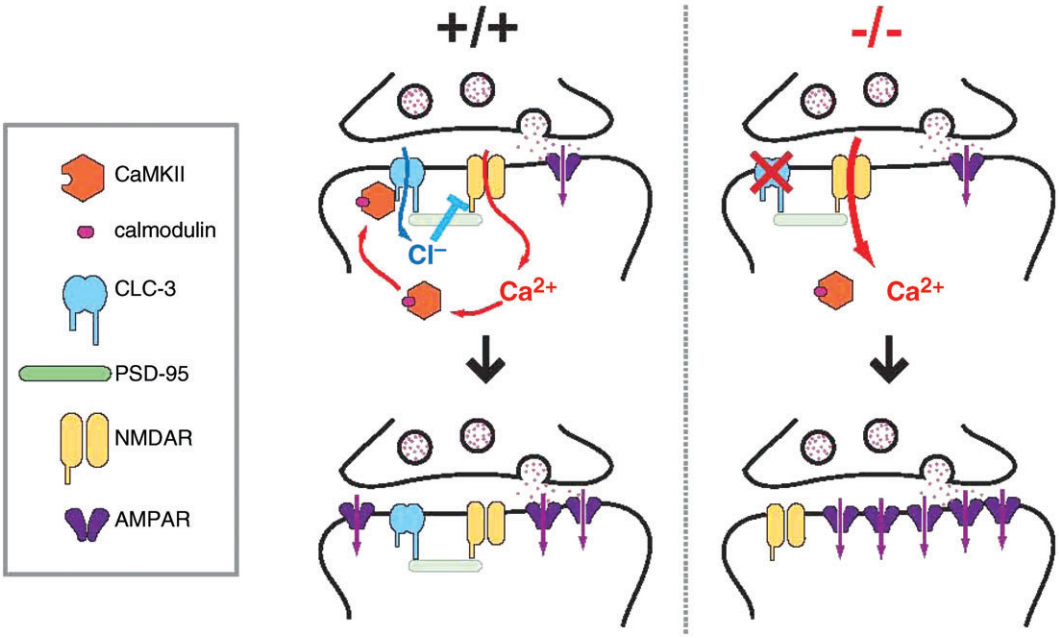

Figure 7. Model of CLC-3 regulation of LTP
Left side, at a WT synapse in a mature animal, Ca^{2+} influx through the NMDAR activates CaMKII, which subsequently phosphorylates/gates CLC-3. The Cl^- flux through CLC-3 results in shunting of membrane potential, reduces depolarization and promotes Mg^{2+} block of the NMDAR, thereby exerting negative feedback on the Ca^{2+} transient at the synapse. This moderates the amount of potentiation that the synapse undergoes. Right side, at a *Clcn3*$^{-/-}$ synapse, there is no regulation of Ca^{2+} influx through NMDARs by CLC-3. This leads to addition of excessive AMPA receptors (or changes in AMPA receptor conductance or distribution) and thus greater LTP for an equivalent stimulus.

contribution of CLC-3 reduces synaptic potentiation on average by ∼43%. The addition of CLC-3 Cl^- inhibition more than compensates for the loss of SK channels, and probably also diminishes the LTP-induced changes in AMPA receptor distribution (as illustrated in Fig. 7) or biophysical properties. Further experiments will be required to identify the exact effects of CLC-3 gating on AMPA receptors.

Long-term potentiation in young animals is dependent on protein kinase A (Yasuda *et al.* 2003), not CaMKII as extensively documented in adult preparations (Malenka *et al.* 1989; Lisman *et al.* 2002). In fact, CaMKII is expressed at somewhat reduced levels until the third postnatal week (Kelly & Vernon, 1985), but this does not appear to lessen CLC-3 function. Wang *et al.* (2006) measured a significant effect of CLC-3 expression on miniature EPSPs in immature cultured neurons consistent with a depolarizing Cl^- gradient at that age. As a result of this developmental switch in kinase dependence of LTP, pinpointing the role of CLC-3 in LTP in immature preparations is complex. However, in combination with previous results, our data predict an opposite effect of CLC-3 in the early postnatal brain in comparison to juvenile and adult brains.

In addition to its postsynaptic function in plasticity, CaMKII is involved in the regulation of presynaptic release (Wang, 2008; Pang *et al.* 2010); application of a CaMKII inhibitor reduces presynaptic function (Waxham *et al.* 1993; Sanhueza *et al.* 2007). Vesicular CLC-3 has also been shown to influence presynaptic function. In inhibitory vesicles particularly, CLC-3 serves as the primary charge shunt pathway to facilitate vesicle acidification and transmitter loading, manifested in the *Clcn3*$^{-/-}$ as a significant decrease in miniature IPSC amplitude (Riazanski *et al.* 2011). In excitatory vesicles, CLC-3 appears to play a lesser role in acidification due to an apparent Cl^- flux through the glutamate transporter VGLUT (Schenck *et al.* 2009). Further confounding the role of CLC-3, the original characterization of the *Clcn3*$^{-/-}$ mouse showed that loading of glutamate is severely compromised in *Clcn3*$^{-/-}$ vesicles, but this is accompanied by an increase in miniature EPSC amplitudes (Stobrawa *et al.* 2001). These inconsistent observations could be explained by an increase in postsynaptic responsiveness, resulting from loss of plasma membrane CLC-3, that conceals reduced glutamate loading. The consequences of plasma membrane chloride channel loss are further obscured by the common convention of setting $E_{Cl} = 0$ mV by equalizing $[Cl^-]$ in the bath and pipette solutions. Although this convention simplifies recordings, it alters the endogenous Cl^- gradient and results in inconsistencies between whole-cell and extracellular recordings which maintain endogenous $[Cl^-]_i$.

Generally, the amount of PPF is inversely related to initial vesicle release probability (Dobrunz & Stevens, 1997; Zucker & Regehr, 2002; Sun & Dobrunz, 2006). Considering this, it is possible that CaMKII acts through CLC-3 to promote vesicle release, raising initial release probability and dampening the amount of PPF. If this were the case, we would expect application of the decoy Tat-CLC-$3_{107-116}$ peptide to increase WT PPF to that of *Clcn3*$^{-/-}$ levels, but we did not observe this; presynaptic release properties tracked with the genotype of the preparation, unaffected by Tat-peptide application (Fig. 6*B*). These results may be explained by a secondary structural function of CLC-3, not requiring N-terminal phosphorylation or ion channel activity (Riazanski *et al.* 2011). Given that only a subset of synaptic vesicles contain CLC-3 (Stobrawa *et al.* 2001; Riazanski *et al.* 2011), we consider it improbable that CLC-3 is structurally necessary for adept fusion.

An alternative means of CLC-3 gating from Matsuda *et al.* (2008*a*) showed that CLC-3 can be activated by low extracellular pH, corresponding to intravesicular pH. This supplementary gating mechanism would be particularly practical for a protein involved in shunting charge build-up in acidifying compartments. Our results do not directly address the gating mechanism of vesicular CLC-3 beyond the observation that CaMKII interaction with residues 107–116 of the N-terminus is unlikely to be involved. A more plausible explanation is that the decreased release probability is a global side-effect of chronic CLC-3 loss and Ca^{2+} dysregulation. For example, the increase in postsynaptic efficacy accompanying CLC-3 loss may induce compensatory mechanisms on the presynaptic side in an attempt to equilibrate baseline signalling and avert excitotoxicity.

We propose that Tat-CLC-$3_{107-116}$ titrates kinase activity from the true CLC-3 N-terminus, as suggested by studies using exogenous peptides in an analogous manner (Ahmadian *et al.* 2004; Lin *et al.* 2008), but it may alternatively interfere with the structural changes necessary for gating. We selected residues 107–116 of the N-terminus as the decoy peptide because phosphorylation of S109 has been implicated in CaMKII-dependent gating of the channel; however, the mechanism by which phosphorylation is translated into channel gating is unknown. Future studies into the gating mechanism of CLC-3 will reveal opportunities for more precise control of ion channel activity.

Our data suggest a fundamental difference in pre- and postsynaptic CLC-3 function. In support of this, there are reports of differential localization of CLC-3A and CLC-3B to intracellular compartments and plasma membrane, respectively (Gentzsch *et al.* 2002). CLC-3B contains an extended C-terminus with a PDZ-binding domain that may be involved in the trafficking of CLC-3 to the plasma membrane and/or the recruitment of CaMKII to CLC-3. In support of this, studies in primary cell culture have corroborated interactions between CLC-3B and

PDZ-binding proteins and kinases, including CaMKII, although whether these interactions promote cell surface trafficking remains unclear (Gentzsch *et al.* 2002; Denton *et al.* 2005; Cuddapah & Sontheimer, 2010). Similar to CLC-3, Allen *et al.* (2011) reported functional and spatial partitioning of the short and long isoforms of SK2 channels. Our results contribute a functional segregation between vesicular and membrane CLC-3 that we predict may be a reflection of the underlying difference in isoform structure.

Chloride channels have been associated with neurodegeneration previously. Loss of CLC-7 leads to CA3 neuron degeneration, in addition to lysosomal storage defects and osteopetrosis (Kasper *et al.* 2005). Neurodegeneration, alterations in tonic GABAergic signalling and upregulation of CLC-2 currents have been recorded in CA1 pyramidal cells in an animal model of temporal lobe epilepsy (Ge *et al.* 2011). Our data suggest a mechanism whereby CLC-3 channels are required for Ca^{2+} regulation during induction of plasticity; long-term dysregulation of Ca^{2+} and excessive expression of LTP eventually leads to excitotoxicity and the degeneration of vulnerable tissues. Therefore, CLC-3 Cl^- channel gating during high activity endows the excitatory synapse with a novel form of Cl^--dependent regulation and may provide a protective limit on Ca^{2+} influx.

References

Ahmadian G, Ju W, Liu L, Wyszynski M, Lee SH, Dunah AW, Taghibiglou C, Wang Y, Lu J, Wong TP, Sheng M & Wang YT (2004). Tyrosine phosphorylation of GluR2 is required for insulin-stimulated AMPA receptor endocytosis and LTD. *EMBO J* **23**, 1040–1050.

Ahmed MS & Siegelbaum SA (2009). Recruitment of N-type Ca^{2+} channels during LTP enhances low release efficacy of hippocampal CA1 perforant path synapses. *Neuron* **63**, 372–385.

Albensi BC, Oliver DR, Toupin J & Odero G (2007). Electrical stimulation protocols for hippocampal synaptic plasticity and neuronal hyper-excitability: are they effective or relevant? *Exp Neurol* **204**, 1–13.

Allen D, Bond CT, Lujan R, Ballesteros-Merino C, Lin MT, Wang K, Klett N, Watanabe M, Shigemoto R, Stackman RW Jr, Maylie J & Adelman JP (2011). The SK2-long isoform directs synaptic localization and function of SK2-containing channels. *Nat Neurosci* **14**, 744–749.

Bats C, Groc L & Choquet D (2007). The interaction between Stargazin and PSD-95 regulates AMPA receptor surface trafficking. *Neuron* **53**, 719–734.

Ben-Ari Y (2002). Excitatory actions of GABA during development: the nature of the nurture. *Nat Rev Neurosci* **3**, 728–739.

Ben-Ari Y, Cherubini E, Corradetti R & Gaiarsa JL (1989). Giant synaptic potentials in immature rat CA3 hippocampal neurones. *J Physiol* **416**, 303–325.

Ben-Ari Y, Khazipov R, Leinekugel X, Caillard O & Gaiarsa JL (1997). $GABA_A$, NMDA and AMPA receptors: a developmentally regulated 'ménage à trois'. *Trends Neurosci* **20**, 523–529.

Benke TA, Luthi A, Isaac JT & Collingridge GL (1998). Modulation of AMPA receptor unitary conductance by synaptic activity. *Nature* **393**, 793–797.

Bliss TVP & Collingridge GL (1993). A synaptic model of memory: long-term potentiation in the hippocampus. *Nature* **361**, 31–39.

Bolte S & Cordelieres FP (2006). A guided tour into subcellular colocalization analysis in light microscopy. *Journal of Microscopy* **224**, 213–232.

Bredt DS & Nicoll RA (2003). AMPA receptor trafficking at excitatory synapses. *Neuron* **40**, 361–379.

Collingridge GL, Isaac JT & Wang YT (2004). Receptor trafficking and synaptic plasticity. *Nat Rev Neurosci* **5**, 952–962.

Cuddapah VA & Sontheimer H (2010). Molecular interaction and functional regulation of ClC-3 by Ca^{2+}/calmodulin-dependent protein kinase II (CaMKII) in human malignant glioma. *J Biol Chem* **285**, 11188–11196.

Denton J, Nehrke K, Yin X, Morrison R & Strange K (2005). GCK-3, a newly identified Ste20 kinase, binds to and regulates the activity of a cell cycle-dependent ClC anion channel. *J Gen Physiol* **125**, 113–125.

Derkach V, Barria A & Soderling TR (1999). Ca2+/calmodulin-kinase II enhances channel conductance of α-amino-3-hydroxy-5-methyl-4-isoxazolepropionate type glutamate receptors. *Proc Natl Acad Sci U S A* **96**, 3269–3274.

Dickerson LW, Bonthius DJ, Schutte BC, Yang B, Barna TJ, Bailey MC, Nehrke K, Williamson RA & Lamb FS (2002). Altered GABAergic function accompanies hippocampal degeneration in mice lacking ClC-3 voltage-gated chloride channels. *Brain Res* **958**, 227–250.

Dobrunz LE & Stevens CF (1997). Heterogeneity of release probability, facilitation, and depletion at central synapses. *Neuron* **18**, 995–1008.

Ge YX, Liu Y, Tang HY, Liu XG & Wang X (2011). ClC-2 contributes to tonic inhibition mediated by α5 subunit-containing $GABA_A$ receptor in experimental temporal lobe epilepsy. *Neuroscience* **186**, 120–127.

Gentzsch M, Cui L, Mengos A, Chang X, Chen J & Riordan J (2002). The PDZ-binding chloride channel ClC-3B localizes to the Golgi and associates with CFTR-interacting PDZ proteins. *J Biol Chem* **278**, 6440–6449.

Green M & Loewenstein PM (1988). Autonomous functional domains of chemically synthesized human immunodeficiency virus tat *trans*-activator protein. *Cell* **55**, 1179–1188.

Huang P, Liu J, Di A, Robinson NC, Musch MW, Kaetzel MA & Nelson DJ (2001). Regulation of human CLC-3 channels by multifunctional Ca^{2+}/calmodulin-dependent protein kinase. *J Biol Chem* **276**, 20093–20100.

Jentsch TJ, Poet M, Fuhrmann JC & Zdebik AA (2005). Physiological functions of CLC Cl^- channels gleaned from human genetic disease and mouse models. *Annu Rev Physiol* **67**, 779–807.

Jin X, Huguenard JR & Prince DA (2005). Impaired Cl^- extrusion in layer V pyramidal neurons of chronically injured epileptogenic neocortex. *J Neurophysiol* **93**, 2117–2126.

Kasper D, Planells-Cases R, Fuhrmann JC, Scheel O, Zeitz O, Ruether K, Schmitt A, Poet M, Steinfeld R, Schweizer M, Kornak U & Jentsch TJ (2005). Loss of the chloride channel ClC-7 leads to lysosomal storage disease and neurodegeneration. *EMBO J* **24**, 1079–1091.

Kauer JA, Malenka RC & Nicoll RA (1988). NMDA application potentiates synaptic transmission in the hippocampus. *Nature* **334**, 250–252.

Kawasaki M, Uchida S, Monkawa T, Miyawaki A, Mikoshiba K, Marumo F & Sasaki S (1994). Cloning and expression of a protein kinase C-regulated chloride channel abundantly expressed in rat brain neuronal cells. *Neuron* **12**, 597–604.

Kelly PT & Vernon P (1985). Changes in the subcellular distribution of calmodulin-kinase II during brain development. *Brain Res* **350**, 211–224.

Kerchner GA & Nicoll RA (2008). Silent synapses and the emergence of a postsynaptic mechanism for LTP. *Nat Rev Neurosci* **9**, 813–825.

Lee HH, Deeb TZ, Walker JA, Davies PA & Moss SJ (2011). NMDA receptor activity downregulates KCC2 resulting in depolarizing $GABA_A$ receptor-mediated currents. *Nat Neurosci* **14**, 736–743.

Lee HK, Takamiya K, Han JS, Man H, Kim CH, Rumbaugh G, Yu S, Ding L, He C, Petralia RS, Wenthold RJ, Gallagher M & Huganir RL (2003). Phosphorylation of the AMPA receptor GluR1 subunit is required for synaptic plasticity and retention of spatial memory. *Cell* **112**, 631–643.

Lee SJ, Escobedo-Lozoya Y, Szatmari EM & Yasuda R (2009). Activation of CaMKII in single dendritic spines during long-term potentiation. *Nature* **458**, 299–304.

Lin MT, Luján R, Watanabe M, Adelman JP & Maylie J (2008). SK2 channel plasticity contributes to LTP at Schaffer collateral–CA1 synapses. *Nat Neurosci* **11**, 170–177.

Lisman J, Schulman H & Cline H (2002). The molecular basis of CaMKII function in synaptic and behavioural memory. *Nat Rev Neurosci* **3**, 175–190.

Lynch G, Larson J, Kelso S, Barrionuevo G & Schottler F (1983). Intracellular injections of EGTA block induction of hippocampal long-term potentiation. *Nature* **305**, 719–721.

Malenka RC, Kauer JA, Perkel DJ, Mauk MD, Kelly PT, Nicoll RA & Waxam MN (1989). An essential role for postsynaptic calmodulin and protein kinase activity in long-term potentiation. *Nature* **340**, 554–557.

Malenka RC, Kauer JA, Zucker RS & Nicoll RA (1988). Postsynaptic calcium is sufficient for potentiation of hippocampal synaptic transmission. *Science* **242**, 81–84.

Malenka RC & Nicoll RA (1993). NMDA-receptor-dependent synaptic plasticity: multiple forms and mechanisms. *Trends Neurosci* **16**, 521–527.

Matsuda JJ, Filali MS, Collins MM, Volk KA & Lamb FS (2008*a*). The ClC-3 Cl^-/H^+ antiporter becomes uncoupled at low extracellular pH. *J Biol Chem* **285**, 2569–2579.

Matsuda JJ, Filali MS, Volk KA, Collins MM, Moreland JG & Lamb FS (2008*b*). Overexpression of CLC-3 in HEK293T cells yields novel currents that are pH dependent. *Am J Physiol Cell Physiol* **294**, C251–C262.

Matsuo N, Reijmers L & Mayford M (2008). Spine-type-specific recruitment of newly synthesized AMPA receptors with learning. *Science* **319**, 1104–1107.

Ngo-Anh TJ, Bloodgood BL, Lin M, Sabatini BL, Maylie J & Adelman JP (2005). SK channels and NMDA receptors form a Ca^{2+}-mediated feedback loop in dendritic spines. *Nat Neurosci* **8**, 642–649.

Ogura T, Furukawa T, Toyozaki T, Yamada K, Zheng Y, Katayama Y, Nakaya H & Inagaki N (2002). ClC-3B, a novel ClC-3 splicing variant that interacts with EBP50 and facilitates expression of CFTR-regulated ORCC. *FASEB J* **16**, 863–865.

Opazo P, Labrecque S, Tigaret CM, Frouin A, Wiseman PW, De Koninck P & Choquet D (2010). CaMKII triggers the diffusional trapping of surface AMPARs through phosphorylation of Stargazin. *Neuron* **67**, 239–252.

Pang ZP, Cao P, Xu W & Sudhof TC (2010). Calmodulin controls synaptic strength via presynaptic activation of calmodulin kinase II. *J Neurosci* **30**, 4132–4142.

Papp E, Rivera C, Kaila K & Freund TF (2008). Relationship between neuronal vulnerability and potassium-chloride cotransporter 2 immunoreactivity in hippocampus following transient forebrain ischemia. *Neuroscience* **154**, 677–689.

Pathak HR, Weissinger F, Terunuma M, Carlson GC, Hsu FC, Moss SJ & Coulter DA (2007). Disrupted dentate granule cell chloride regulation enhances synaptic excitability during development of temporal lobe epilepsy. *J Neurosci* **27**, 14012–14022.

Reisel D, Bannerman DM, Schmitt WB, Deacon RM, Flint J, Borchardt T, Seeburg PH & Rawlins JN (2002). Spatial memory dissociations in mice lacking GluR1. *Nat Neurosci* **5**, 868–873.

Riazanski V, Deriy LV, Shevchenko PD, Le B, Gomez EA & Nelson DJ (2011). Presynaptic CLC-3 determines quantal size of inhibitory transmission in the hippocampus. *Nat Neurosci* **14**, 487–494.

Robinson NC, Huang P, Kaetzel MA, Lamb FS & Nelson DJ (2004). Identification of an N-terminal amino acid of the CLC-3 chloride channel critical in phosphorylation-dependent activation of a CaMKII-activated chloride current. *J Physiol* **556**, 353–368.

Ronesi JA & Huber KM (2008). Homer interactions are necessary for metabotropic glutamate receptor-induced long-term depression and translational activation. *J Neurosci* **28**, 543–547.

Sanhueza M, McIntyre CC & Lisman JE (2007). Reversal of synaptic memory by Ca^{2+}/calmodulin-dependent protein kinase II inhibitor. *J Neurosci* **27**, 5190–5199.

Schenck S, Wojcik SM, Brose N & Takamori S (2009). A chloride conductance in VGLUT1 underlies maximal glutamate loading into synaptic vesicles. *Nat Neurosci* **12**, 156–162.

Schneider CA, Rasband WS, Eliceiri KW (2012). NIH Image to ImageJ: 25 years of image analysis. *Nature Methods* **9**, 671–675.

Schwarze SR, Ho A, Vocero-Akbani A & Dowdy SF (1999). In vivo protein transduction: delivery of a biologically active protein into the mouse. *Science* **285**, 1569–1572.

Schwarze SR, Hruska KA & Dowdy SF (2000). Protein transduction: unrestricted delivery into all cells? *Trends Cell Biol* **10**, 290–295.

Shi SH, Hayashi Y, Petralia RS, Zaman SH, Wenthold RJ, Svoboda K & Malinow R (1999). Rapid spine delivery and redistribution of AMPA receptors after synaptic NMDA receptor activation. *Science* **284**, 1811–1816.

Stobrawa SM, Breiderhoff T, Takamori S, Engel D, Schweizer M, Zdebik AA, Bosl MR, Ruether K, Jahn H, Draguhn A, Jahn R & Jentsch TJ (2001). Disruption of ClC-3, a chloride channel expressed on synaptic vesicles, leads to a loss of the hippocampus. *Neuron* **29**, 185–196.

Sun HY & Dobrunz LE (2006). Presynaptic kainate receptor activation is a novel mechanism for target cell-specific short-term facilitation at Schaffer collateral synapses. *J Neurosci* **26**, 10796–10807.

Wang XQ, Deriy LV, Foss S, Huang P, Lamb FS, Kaetzel MA, Bindokas V, Marks JD & Nelson DJ (2006). CLC-3 channels modulate excitatory synaptic transmission in hippocampal neurons. *Neuron* **52**, 321–333.

Wang ZW (2008). Regulation of synaptic transmission by presynaptic CaMKII and BK channels. *Mol Neurobiol* **38**, 153–166.

Waxham MN, Malenka RC, Kelly PT & Mauk MD (1993). Calcium/calmodulin-dependent protein kinase II regulates hippocampal synaptic transmission. *Brain Res* **609**, 1–8.

Whitlock JR, Heynen AJ, Shuler MG & Bear MF (2006). Learning induces long-term potentiation in the hippocampus. *Science* **313**, 1093–1097.

Yasuda H, Barth AL, Stellwagen D & Malenka RC (2003). A developmental switch in the signalling cascades for LTP induction. *Nat Neurosci* **6**, 15–16.

Yoshikawa M, Uchida S, Ezaki J, Rai T, Hayama A, Kobayashi K, Kida Y, Noda M, Koike M, Uchiyama Y, Marumo F, Kominami E & Sasaki S (2002). CLC-3 deficiency leads to phenotypes similar to human neuronal ceroid lipofuscinosis. *Genes Cells* **7**, 597–605.

Zhao Z, Li X, Hao J, Winston JH & Weinman SA (2007). The ClC-3 chloride transport protein traffics through the plasma membrane via interaction of an N-terminal dileucine cluster with clathrin. *J Biol Chem* **282**, 29022–29031.

Zucker RS & Regehr WG (2002). Short-term synaptic plasticity. *Annu Rev Physiol* **64**, 355–405.

Author contributions

L.M.F. and D.J.N. designed the project. L.M.F. interpreted the results and wrote the manuscript. L.M.F. and B.N.L. collected and analysed the data. All authors approved the final version for publication.

Acknowledgements

The authors wish to express their appreciation to Dr Aaron Fox for many helpful conversations during the course of the work and to Dr Fred Lamb at the University of Iowa who provided the *Clcn3*$^{-/-}$ strain. We thank Dr Radmila Sarac and Erwin Gomez for their careful help with the manuscript and Dr Ivan Goussikov and Erwin Gomez for technical advice. Much gratitude is due to Stephanie Klenotich for her help in making cryosections and to Dr Christine Labno for her imaging expertise. L.M.F. was supported by T32 GM07839-30 and NIH F31 NS076226. The study was supported by NIH R01 GM36823 and NIH R01 DK080364 to D.J.N.